

# Photoconduction of aliphatic polyrhodanines

R. Hirohashi, Y. Toda and Y. Hishiki

Faculty of Engineering, Chiba University, Chiba-shi, Japan

(Received 17 August 1976; revised 17 January 1977)

The photoconductive properties of a series of aliphatic polyrhodanines, prepared from bisrhodanine with dialdehydes, have been measured using a surface-type cell. The temperature dependence of the conductivities of these polymers corresponded to an activation energy of conduction of 0.1–6.2 eV. The electrical resistivity and the activation energy for photoconduction increased with increase in the number of methylene groups in the chain separating rhodanine groups. The large variations in the electrical properties were found to depend mainly on the length of the polymethylene chain between rhodanine groups in the polymer. In unsensitized systems, maximum photoefficiency for photo-current production showed a peak in the photocurrent spectrum occurring at about 554  $\mu\text{m}$  for a number of these polymers.

## INTRODUCTION

Many investigators have studied the photoconduction of polymers containing heterocyclic groups<sup>1</sup>. It has been widely noted that polyvinylcarbazole, which shows a considerable photoresponse, is influenced by various sensitizers<sup>2,3</sup>. Relatively little work has been done on photoconductive behaviour in relation to polymer structure<sup>4,5</sup>. The main interest during the last few years has centred on the photoconductive properties of amorphous thermal stable polymers containing the heterocyclic groups<sup>6</sup>.

In the present work polymers with heterocyclic groups in the main chain were synthesized easily by polycondensation between rhodanines and aliphatic aldehyde in highly polar solvents<sup>7</sup>. The electric field strength dependence of photocurrent and dark current on the length of the methylene chains in a series of aliphatic polyrhodanines has been investigated. The activation energies for dark conduction and photoconduction were measured using a surface-type cell.

## EXPERIMENTAL

### Materials

Seven aliphatic polyrhodanines were prepared by polycondensation of bisrhodanines with dialdehydes (terephthal aldehyde, glyoxal and glutaraldehyde). Aliphatic bisrhodanines were synthesized through the dithiocarbamic acid salt obtained by reaction with aliphatic diamine, carbon disulphide and ammonia or potassium hydroxide. *Figure 1* shows the reaction scheme.

The structure of the polymers was confirmed by comparing the infra-red and ultra-violet spectra with these models corresponding to the unit structure of the polymer. The structure of polyrhodanines has already been established<sup>8</sup>. Elemental analyses agreed with the values calculated for the polyrhodanines. The yields of aliphatic bisrhodanines decreased with increasing length of the methylene chain, because of a pronounced decrease of solubility of the diamine in water (method A). When DMF was used instead of water, and potassium salt instead of the ammonium salt of dithiocarbamic acid, good yields were obtained for deca-(DBR)

and dodeca-methylene (D<sub>0</sub>BR) respectively (method B).

Aliphatic polyrhodanines containing a rhodanine ring in the main chain were synthesized by polycondensation with bisrhodanine (0.01 mol) and terephthal aldehyde (TPA) (0.01 mol) in DMF (50 ml) using triethylamine or pyridine as catalyst at 130°C. Most of the polymers were precipitated during the reaction. When glyoxal (GO) and glutaralde-

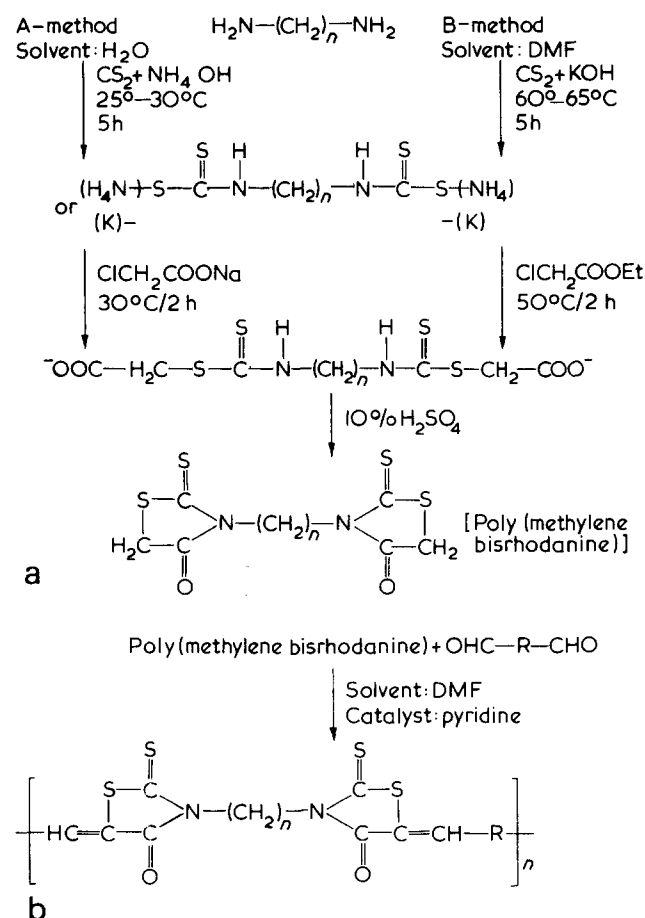


Figure 1 Syntheses of monomers (a) and polymers (b)

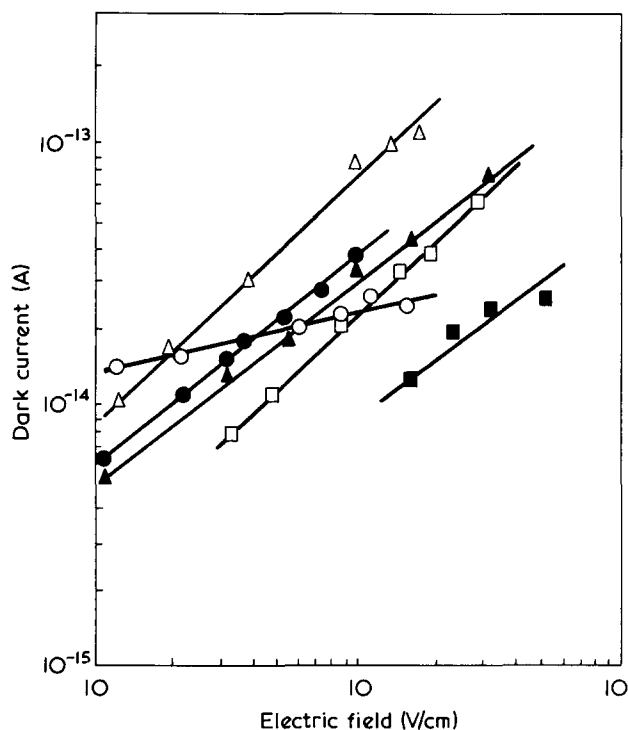


Figure 2 Surface dark current vs. applied electric field for aliphatic polyrhodanines (at  $10^{-6}$  mmHg).  $\circ$ , polymer 1, EBR-TPA;  $\bullet$ , polymer 2, TBR-TPA;  $\triangle$ , polymer 3, HBR-TPA;  $\blacktriangle$ , polymer 5, D<sub>0</sub>BR-TPA;  $\blacksquare$ , polymer 6, EBR-GO;  $\square$ , polymer 7, EBR-GA. EBR, ethylene bisrhodanine; TPA, terephthal aldehyde; TBR, trimethylene bisrhodanine; HBR, hexamethylene bisrhodanine; D<sub>0</sub>BR, dodecamethylene bisrhodanine; GO, glyoxal; GA, glutaraldehyde

hyde (GA) were used instead of TPA, polyrhodanine was precipitated by pouring into acetone. The yellowish polymers were washed for about 48 h with boiling acetone, for 24 h with water and dried in vacuum.

#### Photoconductivity of polymer

The photocurrent was measured by the so-called 'surface cell' method. In all experiments a sample tablet (13 mm in diameter, 1.31 cm<sup>2</sup> surface area and  $\sim 0.5$  mm thick) was moulded by the compression of about 100 mg of a finely powdered specimen at about 200 kg/cm<sup>2</sup>. Silver electrodes were vacuum evaporated in the form of a comb with a 1 mm gap and length of 36 mm on the surface of the pellets. The cell thus obtained was then placed in a closed glass chamber, evacuated to  $10^{-5}$  mmHg, in order to remove water and other volatile impurities.

A 750 W lamp was passed through the quartz window of the cell for measuring the photocurrent. The glass chamber was completely shielded with aluminium foil to exclude all noise. Potentials were applied by dry batteries. Portions of the visible spectrum were isolated with a metallic interference filter. The measured values were correlated with the intensity of the incident light observed by means of a thermopile. The temperature of the sample was not increased on radiation, and in all experiments a heat absorbing filter was used. This fact was confirmed by setting a thermocouple in place of the sample.

Experiments show that some time after the commencement of illumination a constant (steady-state) photoconductivity is established, corresponding to steady-state values of the non-equilibrium carrier densities. The rates of generation of free carriers and of carrier annihilation must be equal when the steady state is reached. The steady-state photo-

current,  $I_p$ , is defined as the difference between the current observed with and without illumination. All dark currents and photocurrents were measured in the steady state, and current-temperature measurements were made by raising the temperature in small steps, and recording the current after steady-state conditions were regained.

The activation energies of conductivity were measured at temperatures ranging from room temperature up to about 160°C. Studies were not carried out at higher temperatures because of the decomposition of the samples. The currents flowing through the samples were in the range  $10^{-12}$ – $10^{-14}$  A and were measured with a Hewlett-Packard micromicroammeter. The micromicroammeter was connected by a well-insulated lead to one electrode attached to the crystal, and the other electrode was connected to dry batteries. The applied voltage varied from 6 to about 120 V.

## RESULTS AND DISCUSSION

#### Structure dependence for dark current

The specific resistivity of aliphatic polyrhodanines at room temperature was in the range  $10^{12}$ – $10^{15}$   $\Omega$ cm. For most of these polymers, the dark current  $I_d$  is directly proportional to the applied voltage  $V$ , and obeys either  $I_d = kV^\alpha$  or  $I_d = kF^\alpha$ , where  $F$  is the electric field strength in V/cm. The dark current of typical samples is shown in Figure 2 as a function of the electric field to the surface-type cell. The variation of dark current with voltage is nearly through the point of origin, showing that the dark current of the specimens obeys Ohm's law except for polymer 1. It may therefore be assumed that the contacts between the sample and the silver electrode are perfect.

The dark current also shows a space charge effect. After switching on the field, the current rises to a peak value which then slowly decreases to equilibrium. When the field is removed, a back current is obtained. The decay of dark current after application of a voltage may be related to dipolar relaxation, tunnelling to empty traps, charge injection leading to trapped space charge effects, and electrode polarization. Dipolar orientation occurs within the material itself, and thus there should be no contact effects. The current is assumed to be a polarization current which decreases rather quickly with time.

Each current-temperature measurement involved raising the temperature in small steps. The time required to reach equilibrium decreases with increasing temperature. The number of electrons released per unit from traps will gradually increase, and when the number of such electrons becomes equal to the number of electrons captured by traps, equilibrium will be realized and the steady current will begin to flow. When the steady state is maintained, the number of electrons falling into traps per unit time will be equal to the number of electrons escaping from traps.

A variety of mechanisms have been invoked to explain the observed conductivity characteristics: for example, Schottky emission<sup>9</sup>, space charge limited current<sup>10</sup>, the Poole-Frenkel effect<sup>11</sup> and impurity interpretation. Electron tunnelling into a discrete trapping level in the dielectric has recently been invoked to account for the absorption current time dependence and the space charge build-up<sup>12</sup>. The linear conjugated system is probably the most generally recognized structural parameter in this field of research. In addition, the degree of  $\pi$ -orbital overlap along a hetero ring has been the most important structural characteristic.

The variation of dark current with polymer structure

Table 1 Chemical structure dependence of the photoconduction of aliphatic polyrhodanines  $-X-(CH_2)_n-X-$ , where X is rhodanine

Structure of methylene chain in polymer	$-(CH_2)_3-$	$-(CH_2)_2-$	$-(CH_2)_6-$	$-(CH_2)_{10}-$	$-(CH_2)_{12}-$
Photo current (A)	$3.5 \times 10^{-11}$	$2.7 \times 10^{-11}$	$5.9 \times 10^{-12}$	$3.7 \times 10^{-12}$	$2.7 \times 10^{-12}$
Structure of methylene chain in polymer	$-(CH_2)_2-$	$-(CH_2)_6-$	$-(CH_2)_3-$	$-(CH_2)_{10}-$	$-(CH_2)_{12}-$
Dark current (A)	$1.3 \times 10^{-14}$	$8.0 \times 10^{-15}$	$5.7 \times 10^{-15}$	$5.7 \times 10^{-15}$	$4.8 \times 10^{-15}$
$I_{photo}/I_{dark}$	$-(CH_2)_3-$ 6130	$-(CH_2)_2-$ 2080	$-(CH_2)_{10}-$ 770	$-(CH_2)_6-$ 740	$-(CH_2)_{12}-$ 560

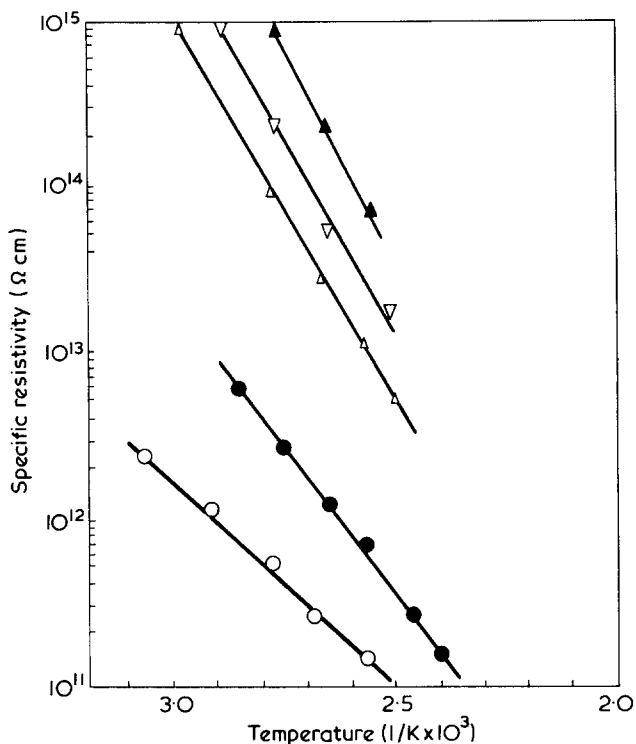


Figure 3 Relationships between specific resistivities and  $1/T$  for aliphatic polyrhodanines: ○, polymer 1, EBR-TPA; ●, polymer 2, TBR-TPA; △, polymer 3, HBR-TPA; ▽, polymer 4, DBR-TPA; ▲, polymer 5, D<sub>0</sub>BR-TPA

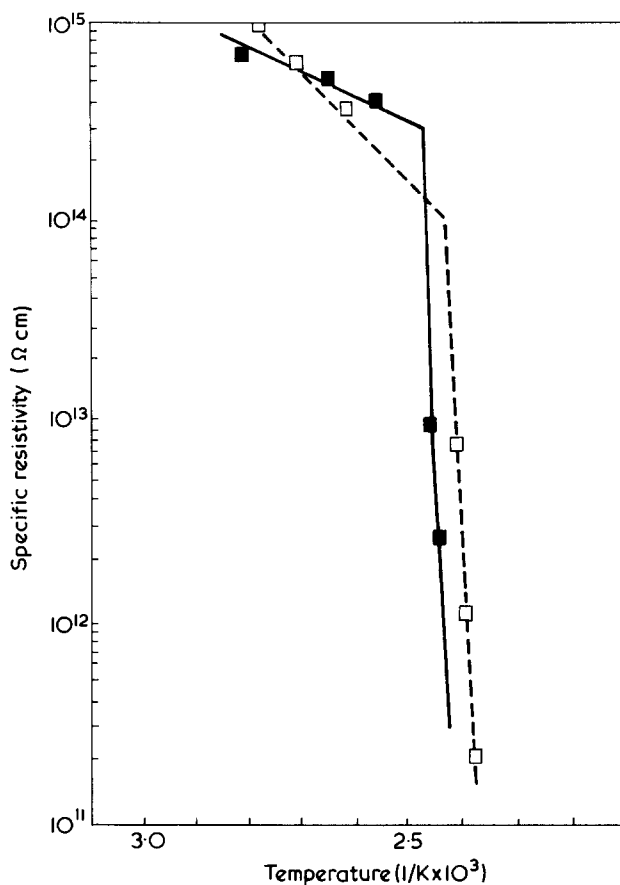
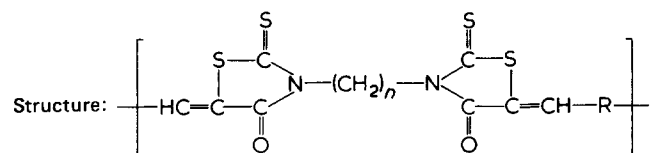


Figure 4 Relationships between specific resistivities and  $1/T$  for aliphatic polyrhodanines: ■, polymer 6, EBR-GO; □, polymer 7, EBR-GA

Table 2 Semiconducting properties of aliphatic polyrhodanines



Exp.	n	-R-	$\eta_{inh}^{30^\circ}$	Temperature range (°C)	Activation energy (eV)
1	2	TPA <sup>c</sup>	0.35	53-117	0.47
2	3	TPA	0.31	55-131	0.68
3	6	TPA	0.19	50-127	0.92
4	10	TFA	0.10	50-100	1.14
5	12	TPA	0.24	100-160	0.53
6	2	GO <sup>d</sup>	0.08	38-105	1.18
7	2	GA <sup>e</sup>	0.05	81-126	0.10
				126-140	6.2
				80-135	0.42
				135-155	6.1

<sup>a</sup> Inherent viscosity; measured at a concentration of 0.2 g in concentrated sulphuric acid (100 ml) at 30°C; <sup>b</sup> activation energy was calculated from linear relationship between  $\log \rho$  and  $1/T$  by the equation  $\rho = \rho_0 \exp(E_a/kT)$ ; <sup>c</sup> terephthal aldehyde; <sup>d</sup> glyoxal; <sup>e</sup> glutaraldehyde

(Table 1) shows that the current is strongly dependent on the length of the methylene chains. The temperature dependence of the steady-state current obeyed the Arrhenius equations  $\log I = I_0 \exp(E_a/kT)$  or  $\log \rho = \rho_0 \exp(-E_a/kT)$ . Figure 3 shows graphs of  $\log$  specific resistivity ( $\rho$ ) against  $1/T$  for some samples. In a series of aliphatic polyrhodanines prepared from TPA, the electrical resistivity and its activation energy ( $E_a$ ) increased with increasing number of methylene groups in the chain (Table 2).

For the aliphatic polyrhodanines, polymer 6 (EBR-GO) and polymer 7 (EBR-GA), the electrical conductivity above the softening temperature was higher than the values measured at lower temperatures. The drastic change of conductivity shown in Figure 4 coincided with the temperature at which weight loss was observed by thermogravimetric analysis; about 135°C for polymer 7, and about 148°C for polymer 6.

#### Structure dependence for photocurrent

The observed photocurrents were found to be strongly

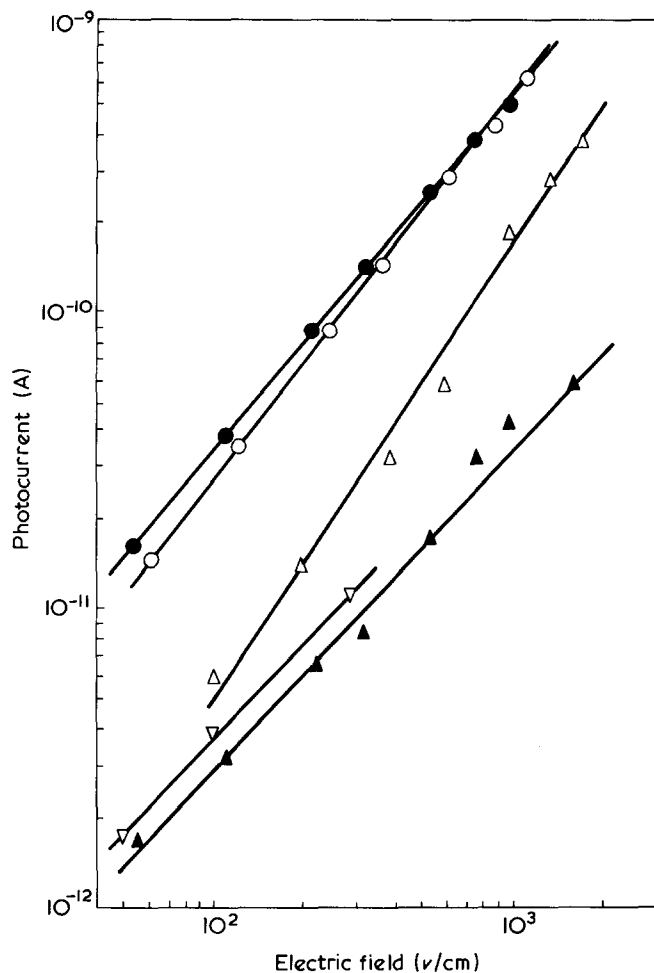


Figure 5 Surface photocurrent vs. applied electric field for aliphatic polyrhodanines illuminated at  $10^{-6}$  mmHg by incandescent tungsten lamp:  $\circ$ , polymer 1, EBR-TPA;  $\bullet$ , polymer 2, TBR-TPA;  $\triangle$ , polymer 3, HBR-TPA;  $\nabla$ , polymer 4, DBR-TPA;  $\blacktriangle$ , polymer 5,  $D_0BR$ -TPA

dependent on a number of variables, the most important of these being: (i) the magnitude of the applied field; (ii) the wavelength and intensity of the incident light; (iii) the state of the illuminated surface; and (iv) the temperature of the sample.

Photocurrent was proportional to electric field strength raised to an exponent higher than unit. Figure 5 shows the results for polymers 1-5 as described in Table 1. The photocurrent rise times and decay times are relatively long, particularly in the red and infra-red regions, and also vary with the wavelength. Thermal heating of the polymer by the illumination employed in these experiments makes a negligible contribution to the current. The order of polymers in relation to the value of their photocurrent is shown in Table 1. The photocurrent will usually depend on the geometry and applied voltage.

The absorption of light changes the distribution of electrons and holes in thermal equilibrium, so that more electrons (or holes) are in free states and the photocurrent is increased. Under steady-state conditions, the disturbance by light is balanced by various recombination processes that tend to return the electrons to their normal equilibrium distribution. When the light source is switched off, the current instantly decreases to the initial dark value. When illuminated with a weak monochromatic light, however, it takes a few minutes to attain the peak current. Also, a

longer time is required for it to reach equilibrium when the light is switched off to neutralize the space charge. The electrons distribute themselves amongst the free states of the conduction band and the traps, and recombination takes place between the free electrons and the fixed holes.

Figures 6 and 7 show graphs of log specific resistivity for photocurrent against  $1/T$  for polymer 1 (EBR-TPA) and polymer 5 ( $D_0BR$ -TPA) respectively for different wavelengths. The values of  $E_a$  evaluated from these plots are listed in Table 3. These energies may include both the energy of carrier formation and the activation energy of carrier migration. The trapping sites will be induced in the molecules in the immediate vicinity of the charged carrier. The charge carriers are, in effect, weakly trapped, the trap depth being proportional to the measured activation energy of photoconduction. If the temperature of the polymer is increased, traps will be destroyed by molecular motion. As the wavelength changes, the thermal activation energy of the photoconduction in the illuminated region increases with decrease of the photon energy. This kind of behaviour cannot be explained in terms of the model of excitation and recombination of charge carriers.

The temperature dependence shows that mobility is an activated process indicating a 'hopping' model or trap controlled bond transport. These activation energies are associated with the charge-carrier transport process. The presence of an activation energy suggests that absorption of a photon does not lead to the direct band-to-band photoexcitation which is observed in many inorganic crystals. These results show that conduction requires two or more steps in the development to a free carrier via a non-conducting initial excited state. Such highly disordered polymers would have many strained bonds that could lead to virtually bound carrier sites.

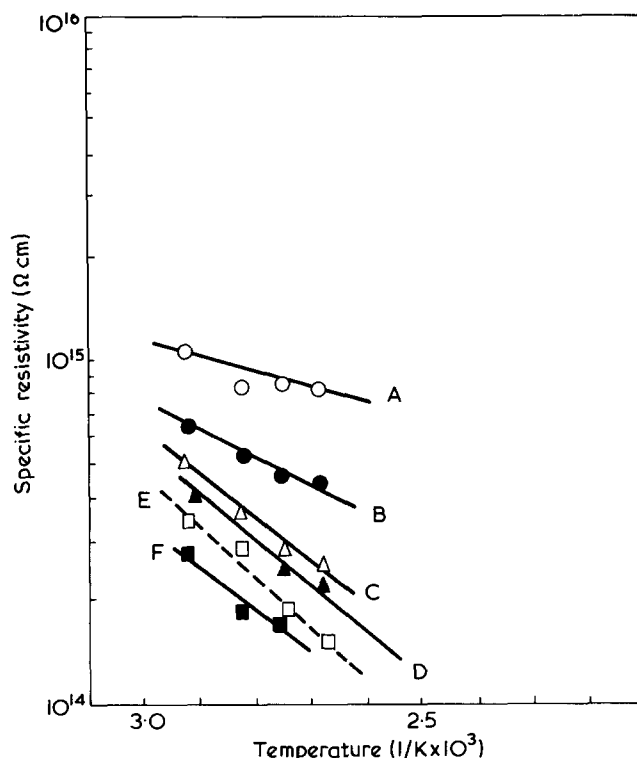


Figure 6 Relationships between specific resistivities and  $1/T$  for each wavelength illuminated for aliphatic polyrhodanines. (polymer 1, EBR-TPA). A, 460; B, 480; C, 550; D, 600; E, 660; F, 680

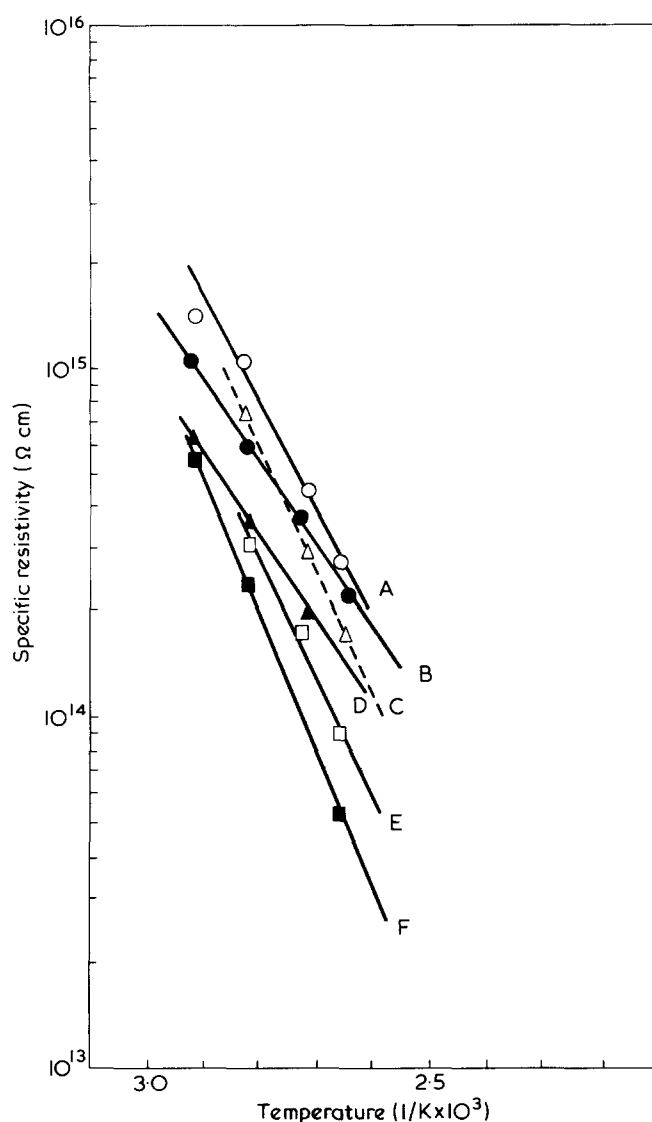


Figure 7 Relationships between specific resistivities and  $1/T$  for each wavelength illuminated for aliphatic polyrhodanines (polymer 5,  $D_0BR-TPA$ ). A, 442; B, 652; C, 602; D, 421; E, 699; F, 555 nm

Table 3 Activation energies of photoconduction in aliphatic polyrhodanines

Polymer 1 (EBR-TPA):						
(nm)	680	660	600	550	480	460
$E_a$ (eV)	0.23	0.29	0.26	0.26	0.15	0.07
Polymer 5 ( $D_0BR-TPA$ ):						
(nm)	699	652	602	555	442	421
$E_a$ (eV)	0.69	0.49	0.69	0.82	0.60	0.48

\*  $E_a$  was calculated from the linear relationship between  $\log \rho$  and  $1/T$  by the equation  $\rho = \rho_0 \exp(E_a/kT)$ ; EBR: ethylene bisrhodanine; TPA: terephthalaldehyde

The large variations in the electrical properties were found to depend mainly on the distances between rhodanine groups in the polymer. The photocurrent of aliphatic polyrhodanines containing  $\sigma$ -bonded methylene groups decreases with increase in the number of methylene groups in the chain. The conformations of the rhodanine ring in the polymer may be important.

The ratio of photocurrent to dark current also decreased

increasing length of the methylene chains (Table 1). The values of  $I_p/I_d$  range from 6130 to 560 and show a strong dependence on the length of methylene chain in polymers. The mobility of the carrier may possibly decrease with the distances between rhodanine groups. The use of polymer 1 and polymer 2 (TBR-TPA) as image materials in electro-photography or similar devices can be envisaged. Structural variations of polyrhodanines may lead to polymers with increased photosensitivity.

#### Spectral dependence of photocurrent

There were indications that certain specimens might be sensitive to near infra-red radiation. Some typical values of photosensitivity against wavelength are given in Figure 8. The intensity of the illumination source was calibrated, thus making it possible to present photoconductivity against wave length data in terms of  $\mu A/W$  of incident light power. Most specimens showed the same maximum response at about 554 nm and 750 nm. The response is not consistent with absorption spectrum data which showed increased absorption at about 465 nm and 285–309 nm. For longer wavelengths the optical absorption coefficient decreases exponentially with wavelength. Quantitatively the thermal activation energy increases, by about the same amount as the corresponding decreases of the photon energy from the absorption edge. This behaviour cannot be explained by the usual model.

When the cell is illuminated with monochromatic light, the photocurrent rises instantly and reaches a maximum value in a few minutes. Also, when the light source is switched off, the current decreases to the initial dark value.

The absorption currents that occurred in polymer dielectrics can in principle be determined by considering the varia-

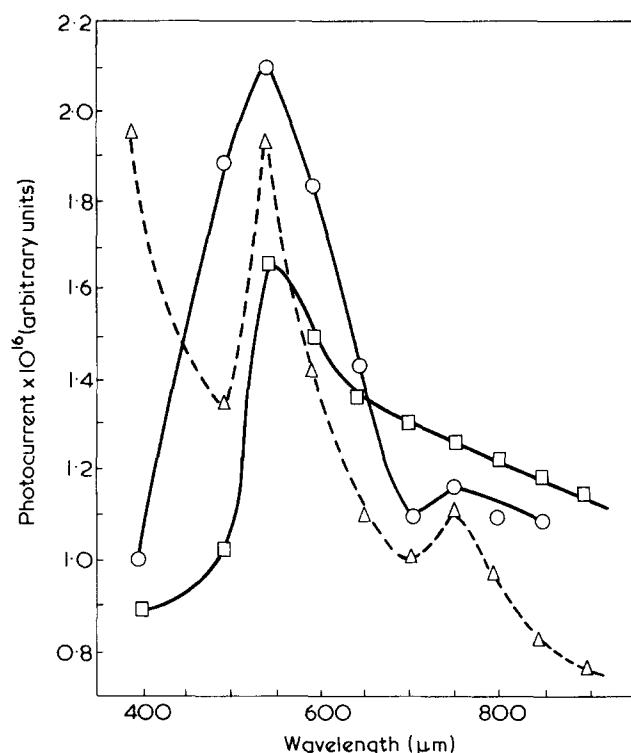


Figure 8 Spectral dependence of the photocurrent of aliphatic polyrhodanines (at  $10^{-6}$  mmHg, by 750 W tungsten lamp with metallic interference filters).  $\circ$ , polymer 1, EBR-TPA, applied voltage 10 V;  $\square$ , polymer 3, HBR-TPA, 100 V;  $\triangle$ , polymer 4, DBR-TPA, 100 V.

tion of transient current with wavelength, temperature, field, thickness and electrode materials. The introduction of carriers by intense light suggests either a direct process by simultaneous absorption of many photons or an indirect process by photo- or thermal ionization of excitons.

#### REFERENCES

- 1 Reucroft, P. J., Scott, H., Kronick, P. L. and Serafin, F. *J. Appl. Polym. Sci.* 1970, **14**, 1361
- 2 Minegishi, T., Kondo, E., Yamanouchi, T. and Kinjo, K. *Z. Phys. Chem.* 1974, **91**, 1
- 3 Meier, H. and Albrecht, W. *Z. Phys. Chem.* 1963, **39**, 247
- 4 Okamoto, Y. and Kundu, S. K. *J. Phys. Chem.* 1973, **77**, 2677
- 5 Hoerhold, H. H. and Opfermann, J. *Makromol. Chem.* 1970, **131**, 105
- 6 Hirohashi, R., Hishiki, Y. and Haruta, M. *Bull. Chem. Soc. Jpn.* 1971, **44**, 2573
- 7 Hirohashi, R., Hishiki, Y., Kojima, A. and Toda, Y. *Nippon Kagaku Kaishi* 1972, **9**, 1718
- 8 Hirohashi, R. and Hishiki, Y. *Kogyo Kagaku Zasshi* 1968, **71**, 1744
- 9 Tomar, V. S. *Solid State Commun.* 1972, **10**, 391
- 10 Pulfrey, D. L., Shousha, A. H. M. and Young, L. *J. Appl. Phys.* 1970, **41**, 2838
- 11 Hayashi, K., Yoshino, K. and Inuishi, T. *Jpn J. Appl. Phys.* 1973, **12**, 1089
- 12 Wintle, H. J. *J. Non-Cryst. Solids* 1974, **15**, 471